

Optimizing Hybrid Metrology through a Consistent Multi-Tool Parameter Set and Uncertainty Model

R. M. Silver^{*a}, B.M. Barnes^a, N.F. Zhang^b, H. Zhou^a, A. Vladár^a, J. Villarrubia^a,
J. Kline^c, D. Sunday^c, and A. Vaid^d

^aSemiconductor & Dimensional Metrology Division, ^bStatistical Engineering Division, and
^cMaterials Science and Engineering Division, National Institute of Standards and Technology,
100 Bureau Drive MS 8212, Gaithersburg, MD, USA 20899-8212; ^dGLOBALFOUNDRIES, 400
Stone Break Road Ext., Malta, NY, USA 12020

ABSTRACT

There has been significant interest in hybrid metrology as a novel method for reducing overall measurement uncertainty and optimizing measurement throughput (speed) through rigorous combinations of two or more different measurement techniques into a single result. This approach is essential for advanced 3-D metrology when performing model-based critical dimension measurements. However, a number of fundamental challenges present themselves with regard to consistent noise and measurement uncertainty models across hardware platforms, and the need for a standardized set of model parameters. This is of paramount concern when the various techniques have substantially different models and underlying physics. In this paper we present realistic examples using scanning electron microscopy, atomic force microscopy, and optical critical dimension (CD) methods applied to sub-20 nm dense feature sets. We will show reduced measurement uncertainties using hybrid metrology on 15 nm CD features and evaluate approaches to adapt quantitative hybrid metrology into a high volume manufacturing environment.

Keywords: optical metrology, electromagnetic simulation, evaluate sensitivities and uncertainties, phase sensitive measurements, through-focus three-dimensional field

1. INTRODUCTION

As critical dimensions (CD) approach 10 nm with the complementary need for sub-nanometer uncertainties that give complete profile or contour information, a new approach is needed, particularly for advanced 3-D model-based metrology. Hybrid metrology has gained significant recognition in a short period of time as an approach to reduce overall measurement uncertainty and optimize measurement throughput while having the potential to yield more complete information [1-9]. The method allows for rigorous combinations of two or more different measurement techniques into a single result. However, regardless of whether the application of the methodology is in a high volume manufacturing (HVM) environment or a metrology lab, a number of fundamental challenges exist in creating a consistent noise and measurement uncertainty model across different hardware platforms, and a similar need exists for a standardized set of model parameters. To put this methodology on a rigorous footing, there must be a consistency in the various techniques, especially when substantially different underlying physical models are used. Reduced measurement uncertainties using hybrid metrology on 10 nm CD features can be demonstrated, but the interpretation of these results is based on details of the methodology used.

Hybrid metrology has recently been shown to directly improve measurement uncertainty introduced through parametric correlation and has further utility in selecting the correct minima among multiple nearby local minima in the fitting space [7]. In this paper we will describe the ability to create a 3-D monolithic representation of a structure where the data reconstruction comes from independent measurements while other attributes are from combined data. The use of parallel regression and *a priori* information through Bayesian statistics entangles the measurement information, even when those parameters or dimensions appear orthogonal. We will explore different parametric combinations to arrive at the most comprehensive 3-D description while minimizing uncertainty through judicious choice of overlapping parameters among different toolsets. Those parameters that overlap provide integrated measurements for those overlapping variables while still influencing the quasi-independent parameters resulting in reduced uncertainties in all

*silver@nist.gov; phone 1 301 975-5609; fax 1 301 975-4299; www.nist.gov/pml/div683/grp02/om3dnm.cfm

parameters. This approach allows the most flexible use of the different measurements to characterize a 3-D target yet also enables flexible strategies to enhance throughput. It is essential however, to develop and contrast this approach in both a high volume manufacturing framework and a metrology laboratory environment, since the uncertainties, throughput and optimization strategies vary significantly.

This technique allows the combination of measurements from model-based instruments such as a scatterometer (optical critical dimension, OCD) as well as standalone measurements with an uncertainty such as those obtained from an atomic force microscope (AFM). When using model-based measurements, a library of curves is assembled through the simulation of a multi-dimensional parameter space. Although parametric correlation, measurement noise, and model inaccuracy lead to measurement uncertainty in the fitting process, these components also lead to the fundamental limitations in the measurement uncertainties. Hybrid metrology provides a strategy to decouple parametric correlation and reduce measurement uncertainties. In the practical application of hybrid metrology amongst multiple tool platforms or models, it is essential to ensure a consistent overlap in the characterization parameters and the uncertainties. The general hybrid metrology framework and flow of data are shown in Fig. 1. To implement a comprehensive, robust framework, it is important to develop a consistent approach to using multiple tools or platforms that have intrinsically different modeling parameters to characterize the structures of interest. We need to develop a rigorous framework using a generalized parameter set that enables each independent measurement method to excel in that unique aspect of a measurement that it performs best so as to provide *a priori* information or regression data with common attributes that maximize utility of the data.

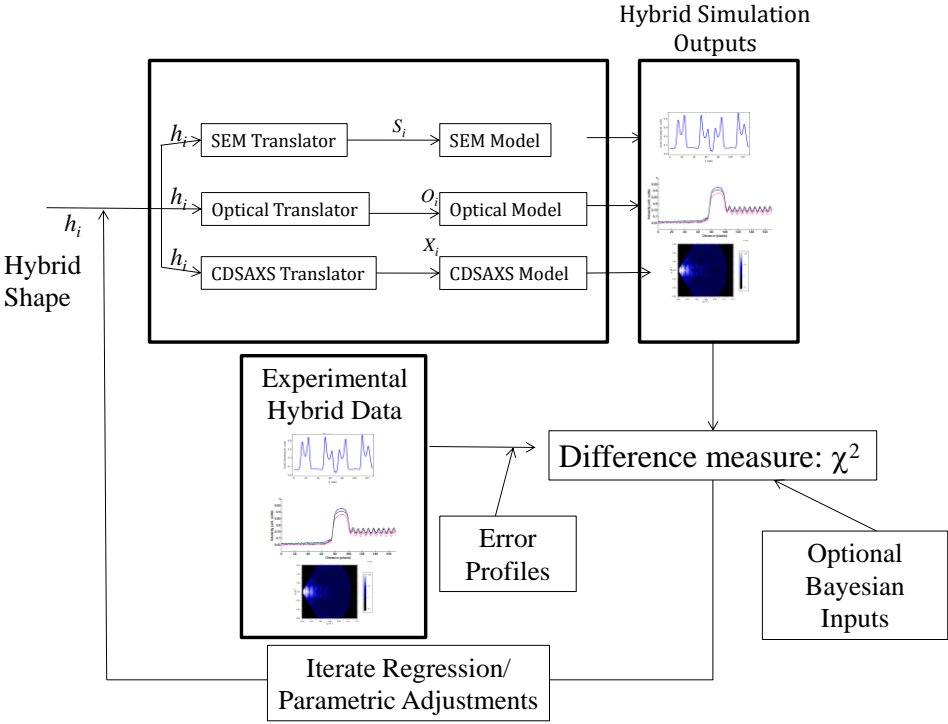


Figure 1. The framework and flow of data in a hybrid metrology example using scanning electron microscopy (SEM), OCD, and critical-dimension small-angle x-ray scattering (CDSAXS). This example allows the use of AFM as a Bayesian input to the parallel regression.

2. CONSISTENT UNCERTAINTY ANALYSIS

One of the key challenges in quantitative hybrid metrology is utilizing consistent noise and uncertainty models across the different platforms. To address this underlying requirement we have developed a rigorous approach to systematic uncertainty evaluation applied across multiple tool platforms. The uncertainty analysis across the various measurement

platforms must comprehensively address the systematic uncertainty components as well as accommodate uncorrected bias or systematic error in the *regression*-based fits.

Although we have described our nonlinear regression in depth previously [7], we briefly introduce the basic math here to discuss the importance of the error models. We have a vector $\mathbf{a} = \{a_1, \dots, a_K\}$ that represents the model input parameters, for example, CD, sidewall angle, height. We have N measured values of Y denoted as $\{y_1, \dots, y_N\}$ and N simulated values $y(x_i; \mathbf{a})$ corresponding to the i^{th} data point x_i . We want to compare the measured $\{y_1, \dots, y_N\}$ with simulated $\{y(x_i; \mathbf{a}), i = 1, \dots, N\}$ and find an optimal estimator of the parameter set $\mathbf{a} = \{a_1, \dots, a_K\}$. Treating $y(x_i; \mathbf{a})$ as a mean response of y_i , we have a nonlinear regression for y_i and $y(x_i, \mathbf{a})$ for $i = 1, \dots, N$ given by

$$y_i = y(x_i, \mathbf{a}) + \varepsilon_i \quad \text{for } i = 1, \dots, N, \quad (1)$$

where ε_i is the corresponding error. Using a first-order Taylor expansion, a linear approximation of the nonlinear regression is given by

$$y_i = y(x_i; \mathbf{a}(0)) + \sum_{k=1}^K \left[\frac{\partial y(x_i; \mathbf{a})}{\partial a_k} \right]_{\mathbf{a}=\mathbf{a}(0)} (a_k - a_k(0)) + \varepsilon_i, \quad (2)$$

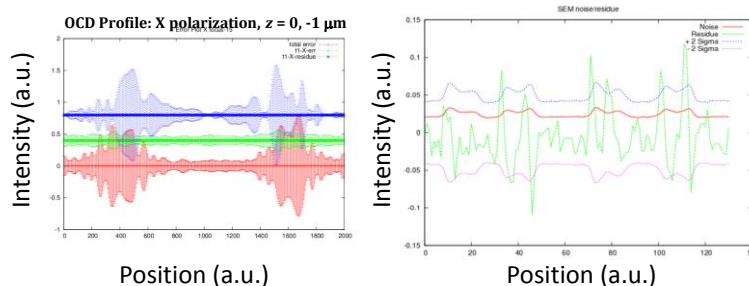
where $\beta = (a_k - a_k(0))$, $\mathbf{a}(0) = \{a_1(0), \dots, a_K(0)\}$ is an initial value or an optimal value of \mathbf{a} , and ε_i is the corresponding error [10]. The ε_i represent the complete error between the experimental value and the simulated value at the i^{th} data point. It is essential to understand that this error component includes all sources of error, both Type A and Type B error estimates. That is, all sources of error including experimental repeatability, hardware errors, and modeling errors.

We need to develop Type A (repeated measurements) and Type B (estimated values) uncertainties for experiment and simulations. To reach a consistent Guide to Measurement Uncertainty (GUM) [11] compliant result, we must use GUM-compliant uncertainty analysis which will then result in traceable combined measurements most suitable for reference metrology. The GUM compliant uncertainty components may be estimated by repeat experimental acquisitions to obtain the Type A estimates, or by other methods (Type B) such as expert estimation, often used for nonrandom errors such as angular alignment, spectral width, tool normalization, illumination angles, symmetry, rotation, etc. We also need to evaluate all modeling errors due to finite grid size, convergence, underlying physics approximations, etc. The error set also includes any discrepancy between the geometrical model and the actual targets measured (rounding, footing...). Ultimately, the Type B errors are combined with experimental Type A repeatability uncertainty components.

While the above description is essential to achieving an accurate GUM compliant result, this approach may prove difficult if not impossible in a current HVM environment. In this situation, we can explore an alternative approach by using a “confidence or influence” factor based on in-house standards, manufacturing variability, reference metrologies such as transmission electron microscopy (TEM), or other gauges to determine the quality of data and associated measurement uncertainties relative to a reference or gauge. This methodology uses Data Modification Parameters (DMP) to modulate the strength and the way data is used during Hybrid Metrology [8].

An example of a GUM compliant, complete uncertainty analysis for a scatterfield OCD measurement is shown on the left in Fig. 2 with a similar SEM error profile shown on the right in the figure. The OCD error profile shows a single focus height error profile. In the scatterfield OCD examples used throughout this paper, the OCD fitting routines use 21 sets of image data from 21 different focus heights for each individual target analysis. In the library regression, all 21 sets of data are simultaneously fit and each focus height has its own unique error profile composed of all of the individual focus-dependent elements described briefly above. In the case of the SEM uncertainty profile, the dominant uncertainty components are due to experimental repeatability, theory to experiment fitting errors and a limited analysis of the hardware errors.

Figure 2. On the left, profiles in red are the complete OCD error maps, green is experimental repeatability and the blue curves show theory to experiment fitting residuals. On the right, an example error profile and residuals for the SEM data.



Once a comprehensive uncertainty analysis is complete for each individual tool, we need to define the parameters to be floated and fit in the individual regressions. Next, we discuss forming the generalized parameter set which serves as the geometrical model input parameters and their interaction within the general flow of a hybrid metrology model.

3. GENERALIZED PARAMETER SETS

Model-based metrology techniques generally require the sample shape to be described by a chosen parameterization. The different values of the parameters describe different members of a family of shapes. Using a least squares fitting routine to evaluate the closeness of the fit between the model output and the measured values, the best-fit member in the family of shapes can be found. Parameterization is inherently an approximation since the shapes in the parameterized family do not exhaust all of the possibilities available to nature. On the one hand, it is desirable to make this approximation as good as possible, a goal that can be furthered by having more free parameters. On the other hand, this must be weighed against the computation cost and potential increase in parametric correlation. If, for example, the effects of two (or more) parameters cannot be distinguished within an instrument’s resolution, correlations between these parameters will render the fitting process more complex with greater uncertainties. For this reason the choice of parameterization is a compromise. Although there remains some art to it, there is a test for success: when a modeled shape fits the measured signal to within that signal’s uncertainty, that shape is indistinguishable from the true shape by the metrology tool.

Parameterizations are not unique. The identical circle, for example, can be specified by its radius, its area, or its circumference. If approximations are permitted, the possibilities increase. Given the freedom implied by this non-uniqueness, and given that different measurement tools have different strengths and weaknesses, it is to be expected that different metrology tools will find different optimal solutions to the compromise described in the previous paragraph. The models developed for the tools each require inputs, and it is common that each method will have its own preferred parameterization. This is illustrated in Fig. 1 by the SEM, Optical, and CDSAXS models accepting inputs S_i , O_i , and X_i respectively. This is one central challenge for hybrid metrology: how to best define a generalized parameterization for all the different techniques that do not necessarily share the same definition of parameters?

A solution to the formation of a generalized shape that can be translated into inputs for each of the individual simulators is indicated in Fig. 1. This involves choosing a shape that is parameterized in a way that each individual method can translate the shape parameters into its own model input parameters and the parameter set for each individual model can be characterized by a goodness of fit metric such as a sum of least squares value with respect to the shape defined by the generalized parameter set. The hybrid tool has its own parameterization, indicated by h_i . As shown in the figure, each individual tool must translate these parameters into its own preferred system. One way to achieve this is shown in Fig. 3. The shape described by a given set of parameters could be rendered into a continuous function, $r(\theta)$, in radial coordinates relative to a reference origin as shown in the left panel or as left and right displacements, $w_l(z)$ and $w_r(z)$, from a vertical reference line as shown in the middle panel. Given a set of parameters, \mathbf{h} , one then translates to \mathbf{S} by choosing the \mathbf{S} that minimize the squared “distance” between the two curves: $\int_0^h [(w_l(z, \mathbf{h}) - w_l(z, \mathbf{S}))^2 + (w_r(z, \mathbf{h}) - w_r(z, \mathbf{S}))^2] dz$. The right panel in Fig. 3 shows an SEM shape with a rounded corner (blue) and a multi-trapezoidal approximation (red). As this example illustrates, because \mathbf{h} and \mathbf{S} represent different attempts to approximate the same underlying shape, it may not be possible to make this distance equal 0. Any remaining difference between the shapes they describe is similar in character to the difference between any parameterized shape and nature’s true shape. Either of

these represents an error in the model, an error which can be considered small enough if the instrument is not sensitive to the small differences between them.

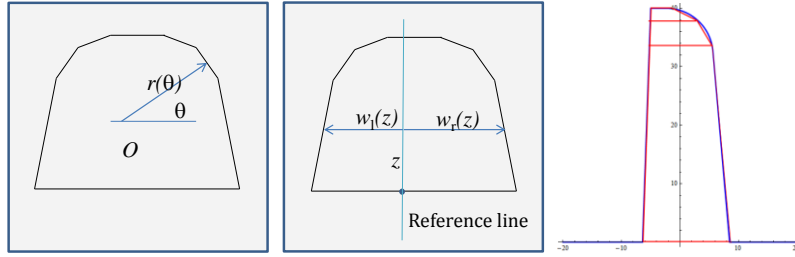


Figure 3. A few examples of potential parameterizations for a general line shape. The shape on the right is a specific input geometry for the SEM which can be characterized by the generalized shapes on the left.

Once the generalized parameterization is defined, a set of shapes can be defined that represents the set of parameters to be floated for each individual model. The transformations from generalized parameters to individual model inputs results in the library of simulation curves that define the total simulation domain of the parameter set. The generalized parameter set resulting in the best fit and the set of shapes about the best fit shape define the individual model inputs needed for calculation of the derivatives in Eqn. 2. Note that not all measurement methods and models need to float or measure all parameter values. Any method may limit its floating model parameters to a subset of the total parameter set as well as limiting those parameters that overlap.

In the experimental examples that follow, the SEM and OCD use trapezoidal parameterizations while the AFM is limited to a top width, middle width, and height. The next section describes sample design in detail as well as the specific OCD and SEM parameterizations used in the simulations presented here.

4. SAMPLE DESIGNS

A series of finite targets were fabricated by SEMATECH that have a designed linewidth variation from target to target similar to a focus exposure matrix, see Fig. 4. Sets of nominally 14 nm, 16 nm, and 18 nm lines were fabricated on the SEMATECH wafers. Target materials are Si on Si with a thin native, conformal oxide. Wafers were fabricated using e-beam lithography so linewidth bias at the edge of the finite arrays is substantially less than typically observed using an optical lithography process. Although there may be some subtle process induced bias at the edges, measurements show that CD edge bias is no larger than the bias across the target. Line extensions were included to facilitate AFM measurements, and again, although it is recognized that some bias will exist here as well between the main field of view and the AFM extensions measurements show it is minimal. One major benefit of the target designs used here is that current target sizes as small as 1.75 μm x 6 μm and potentially smaller can be measured. This is one of the primary benefits of using the scatterfield OCD approach, that small finite targets can be measured.

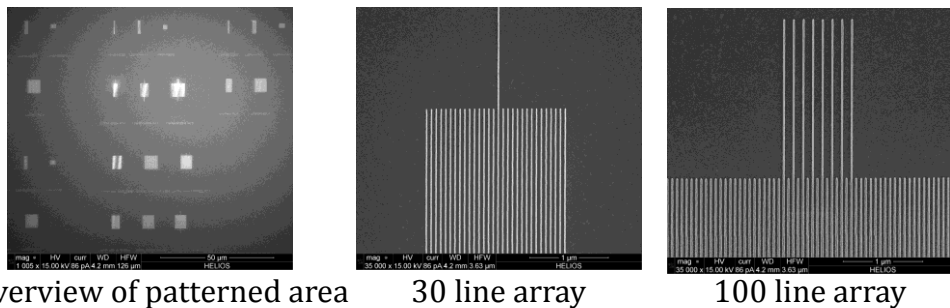


Figure 4. SEM images showing the overall target layout, the 30 line arrays with single AFM extensions and the 100 line finite array with 8 line extensions. Horizontal field of views: 126 μm (left) and 3.63 μm (middle and right)

The geometrical parameterizations used for the two individual model-based methods are shown in Fig. 5. The OCD methods used a 4 trapezoid geometry characterized by a middle width, top width (20 %), and bottom width (80 %), as well as fixed top rounding and bottom footing as seen in the figure. The SEM used a similar “overlapping” geometry set

except the top rounding is in fact actually a curved profile. It is critical for each measurement method to have maximum flexibility in defining the fine details of the parameterization to optimize the individual measurements while maintaining as much generalization as practicable for the hybridization.

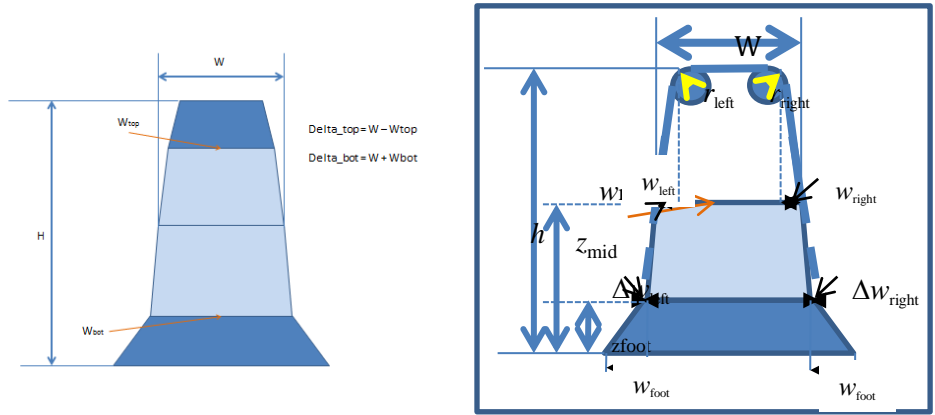


Figure 5. Optical geometrical parameterization and SEM geometrical parameterization.

Following the definition of the generalized shapes and derivative geometries, the next step is to build individual simulation libraries for the separate methods and establish the individual best fit parameters and uncertainties. The individual measurement fits, shown in Table 1, should statistically “overlap.” That is the best fit values and their uncertainties on the geometrical shapes must be consistent within the uncertainty envelopes. This is a key step in hybrid metrology. Obtaining agreement between the individual independent regressions for SEM and OCD along with AFM measurements requires accurate and complete error analysis. For example, in Table 1 the uncertainties for the individual SEM fit does incorporate Type B components placing it on the same footing as the OCD and AFM uncertainties. It should also be noted that the OCD minimum in Table 1 is in fact a local minimum and was chosen over the global minimum as the latter was determined to be an unphysical solution to the regression based on reliable height data from the reference AFM. The χ^2 values should also be near the number of degrees of freedom (indicating a good fit of model to data) for the individual methods before applying the hybridization.

Table 1. Individual fits reported from each measurement technique. Uncertainties in all tables are $k = 1$.

SEM	CD, 0.5 h (nm)	CD top, 0.8 h (nm)	CD bot, 0.2 h (nm)	Height h (nm)
Values	17.01	14.16	19.87	34
Uncert.	0.44	0.31	0.54	fixed

OCD	CD, 0.5 h (nm)	CD top, 0.8 h (nm)	CD bot, 0.2 h (nm)	Height h (nm)
Values	17.30	13.40	18.07	35.08
Uncert.	0.60	0.72	1.33	0.51

AFM	CD, 0.5 h (nm)	CD top, 0.95 h (nm)	CD bot, 0.2 h (nm)	Height h (nm)
Values	18.5	11.3		32.8
Uncert.	1.5	2.0		0.7

5. HYBRIDIZATION FOR SEM, AFM, AND SCATTERFIELD OCD

Once the initial comparisons are complete, the first step in the parallel regression for SEM and Scatterfield OCD involves simulating about the best estimate $\mathbf{a}(0) = \{a_1(0), \dots, a_k(0)\}$ for the combined measurement set. Ultimately this is an iterative process and the best fit will be found, although there are a few different algorithms that can be used to make this iterative fitting process most efficient. Table 2 shows the first iteration simulation sets using a starting 18 nm middle width value, chosen to coincide between the OCD fit and the AFM reference values. The resulting β values are then used with a damping factor to estimate the next iteration and a new set of best fit parameters. These are shown in the uppermost combined data set in Table 3. In these data, the SEM and OCD were combined using two overlapping floating parameters. Again, the χ^2 fits should be consistent across the tool sets with proper measurement uncertainties obtained by combining all tool, model and sample errors. A key result to notice here is the reduced uncertainties in the combined regression result. Also note that all of the uncertainties are affected due to the “entanglement” of the parameters through parametric correlation.

Next, we compare hybridizing the SEM and OCD through parallel regression with the Bayesian combination where the SEM is used as a Bayesian input to the OCD regression. The data in Table 3 show that the parallel regression in fact results in a slightly higher uncertainty compared to the Bayesian input of the same two overlapping parameters. However, this should not be considered significant since in this example, only one iteration in the fitting process was completed, and there is likely a numerical error resulting from using a limited number of iterations. At this point in the combined regression, standard methods for finding a stable minimum in the local space can be used. The final resolution from the combined minimization is generally dependent on the computation resources available to adequately address the non-linearity of the parametric space with a sufficient density of points.

The final segment in Table 3 shows best fit values and uncertainties with the AFM height used as a Bayesian input to the OCD in combination with the SEM/OCD hybrid regression. This example is meant to illustrate the various ways that data from different instrument platforms can be combined or utilized in various sampling or measurement strategies.

Table 2. Initial starting parameters for parallel regression. It should be noted that the parametric uncertainties provided at the initial starting parameters are not calculated at a local minima of either technique’s fitting and therefore are not physical uncertainties.

Starting point values for parallel regression.

SEM	CD (nm)	CD top (nm)	CD bot (nm)	Height (nm)
Values	18.0	15.0		34
Uncert.	0.45	0.83		fixed

OCD	CD (nm)	CD top (nm)	CD bot (nm)	Height (nm)
Values	18	15	19	34
Uncert.	0.60	0.72	1.33	0.51

Table 3. Comparison of SEM and OCD as a parallel regression and as a Bayesian input using the same two, overlapping parameters, as shown in Table 1. The last table shows AFM used as a Bayesian input to the SEM parallel regression.

Parallel Regression: 2 parameters SEM and OCD

SEM and OCD	CD (nm)	CD top (nm)	CD bot (nm)	Height (nm)
Values	17.45	13.67	17.92	34.86
Uncert.	0.36	0.48	0.81	0.33

Bayesian input: 2 parameters SEM into OCD

SEM	CD (nm)	CD top (nm)	CD bot (nm)	Height (nm)
Values	17.45	13.56	17.93	34.93
Uncert.	0.26	0.28	0.60	0.27

Combined parallel regression for SEM and OCD with AFM as Bayesian input to OCD

OCD	CD (nm)	CD top (nm)	CD bot (nm)	Height (nm)
Values	17.69	13.96	17.67	34.58
Uncert.	0.34	0.47	0.75	0.30

6. CONCLUSIONS

We have described a variety of methods to combine measurement results from different tool platforms. This new hybrid metrology strategy has implications in the extensibility of the various individual tool sets from both a throughput and reference metrology standpoint. This new approach is capable of providing a full three dimensional quantitative visualization/representation of the sample. There are also important potential gains using hybrid metrology for optimizing measurement throughput when using time-consuming measurements. This method provides a technique to maximize the utility of SEM or CD-SAXS measurement data by weighing the utility of more accurate high-resolution information versus additional acquisition and analysis time. The method is also well suited to include manufacturing variability into the hybrid model from predictable effects such as process induced variation due to a bake plate or known lithography variability [9].

There are a number of key challenges that remain however, when developing or implementing a quantitative hybrid metrology framework. Real data may not always conform to common statistical assumptions (random, uncorrelated, normally distributed errors, ...), and the effect these departures have on the uncertainty of model parameters is unclear and requires further study. If there are any unrecognized biases in the different measurements, the resulting measurements may not overlap to within their determined uncertainties. In such cases, combining the measurements has the benefit of identifying where further understanding is needed to obtain overlap of the best fit values. This remains an ongoing challenge. We have put substantial effort into making the physical models comprehensive and using thorough uncertainty analysis to achieve statistical overlap in the best fit parameters. It is also important to address sample variability and define a quantitative approach to properly compensate for local versus large field measurements.

There are very important implementation gains with the combination of techniques for reference metrology. The combined uncertainties necessarily result in more accurate reference metrology. However, "methods divergence" is an intrinsic part of hybrid metrology. This must be addressed to achieve quantitative, accurate hybrid metrology. There is also the need to invest in substantial research to develop a comprehensive methodology that fully or best incorporates the rigors of laboratory-based hybrid metrology into a practical factory environment.

REFERENCES

- [1] R. M. Silver, N. F. Zhang, B. M. Barnes, H. Zhou, A. Heckert, R. Dixson, T. A. Germer, and B. Bunday, "Improving optical measurement accuracy using multi-technique nested uncertainties," Proc. SPIE 7272, 727202 (2009).
- [2] N. Rana and C. Archie, "Hybrid reference metrology exploiting patterning simulation", Proc. SPIE 7638 (2010).
- [3] J. Foucher, N. Rana, and C. Dezaudier, "3D-AFM Enhancement for CD Metrology Dedicated to Lithography Sub-28 nm Node Requirements", Proc. SPIE 7638 (2010).
- [4] R. M. Silver, N. F. Zhang, B. M. Barnes, H. Zhou, J. Qin, and R. Dixson, "Nested Uncertainties and Hybrid Metrology to Improve Measurement Accuracy", Proc. SPIE 7971, (2011).
- [5] R. M. Silver, N. F. Zhang, B. M. Barnes, J. Qin, H. Zhou, and R. Dixson, "A Bayesian Statistical Model for Hybrid Metrology to Improve Measurement Accuracy", Proc. SPIE 8083 (2011).
- [6] A. Vaid, et al., "Holistic metrology approach: hybrid metrology utilizing scatterometry, critical dimension-atomic force microscope and critical dimension-scanning electron microscope," Journal of Micro-Nanolithography Mems and Moems 10 (4) (2011).
- [7] N. F. Zhang, R. M. Silver, H. Zhou, and B. M. Barnes, "Improving optical measurement uncertainty with combined multitool metrology using a Bayesian approach," Applied Optics 51 (25), 6196-6206 (2012).
- [8] A. Vaid, et al., "Hybrid metrology solution for 1X node technology", Proc. SPIE 8324 (2012).
- [9] C. J. Spanos, J. Y. Baek, "Enhancing metrology by combining spatial variability and global inference," Proc. SPIE 8681, 86813E (2013).
- [10] J. Neter, W. Wasserman, and M. H. Kutner, [Applied Linear Regression Models], Richard D. Irwin, (1983).
- [11] ANSI/NCSL Z540-2-1997, [Guide to the Expression of Uncertainty in Measurement], NCSL International, (1997).

Certain commercial materials are identified in this paper in order to specify the experimental procedure adequately. Such identification is not intended to imply recommendation or endorsement by the National Institute of Standards and Technology, nor is it intended to imply that the materials are necessarily the best available for the purpose.